Multiphoton Resonance with One to Many Cycles

R. B. Watkins, W. M. Griffith, M. A. Gatzke,* and T. F. Gallagher
Department of Physics, University of Virginia, Charlottesville, Virginia 22901
(Received 13 March 1996)

Using radio frequency pulses we connect the relatively unstructured response of a two level system to a half cycle pulse to the resonant response to a monochromatic wave. There is an obvious change from the nonresonant effect of a half cycle pulse to an interference pattern analogous to a Young's two slit interference pattern with two cycles. The analog of illuminating more slits, adding progressively more cycles, leads to a gradual evolution of the interference maxima into sharp resonances. The structured response to M cycles is implicit in the response to one cycle. [S0031-9007(96)01243-4]

PACS numbers: 32.80.Wr

The evolution of a quantum mechanical system in a strong electric field pulse or in an intense laser pulse containing only a few optical cycles is easily calculated by explicit numerical integration of the Schrödinger equation [1,2]. Since this approach is awkward for descriptions of multiphoton resonance phenomena driven by long, nearly monochromatic pulses of radiation, such processes are often described by Floquet approaches, which have little apparent connection to explicit numerical integration [3,4]. The question of how to connect these two approaches is not academic, since it is now possible to make laser pulses containing only a few optical cycles [5,6].

In fact, the two approaches are intimately related. As pointed out by Moloney and Meath [7], it is a straightforward matter to construct the unitary time evolution operator U by numerical integration over one field cycle. The evolution operator for an M cycle pulse is then simply U^M. In the related problem of above threshold ionization (ATI), Muller [8] has pointed out that even if electrons are freed from atoms only at the peaks of the optical cycles the fact that the electron ejection can occur over many cycles leads to sharp peaks, spaced by the photon energy, in the electron energy spectrum.

Here we report the experimental observation of the response of a two level system to pulses containing from one to fifteen radio frequency (rf) cycles. Specifically, we observe the development of multiphoton resonances with increasing numbers of cycles. We have driven transitions between the potassium 21s and 19,3 states in a static electric field E_s. The 19,3 state is adiabatically connected to the zero field $n = 19$, $\ell = 3$ state. As shown by Fig. 1 the 19,3 state has a large linear Stark shift and an avoided crossing with the 21s state at the static field $E_c = 304.2$ V/cm, where the two states are 339 MHz apart. We drive transitions between the two states by adding an rf field pulse, parallel to the static field, with a chosen number of cycles. As shown in Fig. 1, for $E_s < E_c$ the positive half cycle adds to the static field bringing the states closer to the avoided crossing while the negative half cycle moves the states away from the avoided crossing.

We fix the amplitude $E_{\rm rf}$ and the number of cycles and observe the $21s \rightarrow 19,3$ transition probability as we slowly sweep the static field, which alters the energy separation between the two states. With a long rf pulse this approach yields a clear sequence of multiphoton transitions [9]. With a single cycle the transition probability increases monotonically as $E_s + E_{\rm rf}$, the peak total field, approaches E_c. This dependence can be understood by examining Fig. 2(a), a plot of the energies of the 21s and 19,3 states vs time in a single cycle pulse for static and rf fields such that $E_s + E_{\rm rf} = E_c$. The transition probability arises from the mixing of the two states at the peak of the field, reflected in the deviations of the 21s and 19,3 energies from a constant and a sinusoidal oscillation. For a fixed amplitude $E_{\rm rf}$ with smaller static fields the distortion of the energy levels and the transition probability are lower. When $E_s + E_{\rm rf}$ exceeds E_c the avoided crossing is traversed twice, as shown in Fig. 2(b), and there are two paths by which atoms can go from the 21s to the 19,3 state. These two paths interfere constructively or destructively depending on their phase difference θ, leading to pronounced

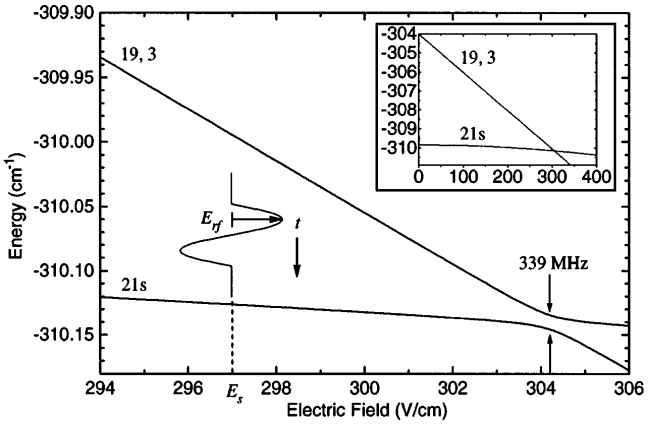

FIG. 1. Energy level diagram showing the K 19,3 and 21s states vs static field E_s (shown in the figure at 297 V/cm). The levels have an avoided crossing at $E_s = E_c = 304.2$ V/cm. For $E_s < E_c$ the positive half cycle of the added rf field brings the atoms to the avoided crossing, as shown by the single cycle of the rf field of amplitude $E_{\rm rf}$.

 0031-9007/96/77(12)/2424(4)$10.00

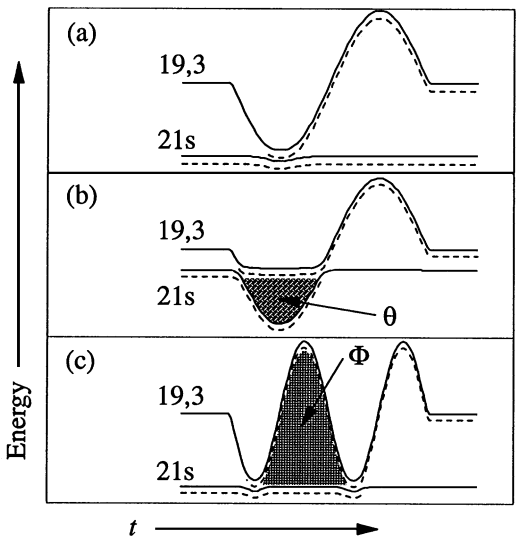

FIG. 2. Temporal variations of the energies of the 21s and 19,3 states showing the evolution starting from an initially populated 21s state in several rf pulses. (a) A single cycle pulse for which $E_s + E_{\rm rf} = E_c$. The single possible $21s \rightarrow 19,3$ path is shown by the broken line. (b) A single cycle pulse for which $E_s + E_{\rm rf} > E_c$. There are two $21s \rightarrow 19,3$ paths, shown by the broken lines, with a phase difference θ between them leading to Stückelberg oscillations. θ is the indicated area between the two paths. (c) A two cycle pulse with $E_s + E_{\rm rf} = E_c$. There are two $21s \rightarrow 19,3$ paths with phase difference Φ leading to intercycle interference, or resonance.

Stückelberg oscillations in the transition probability [1]. As implied by θ in Fig. 2(b), we use atomic units unless others are given explicitly. Our interest here is in the intercycle interference which occurs with more than one rf cycle. Specifically, we have observed changes in the transition probability as progressively more cycles are added. A second cycle introduces a sinusoidal modulation onto the single cycle transition probability, roughly analogous to Young's two slit interference pattern. As more cycles are added the maxima develop into progressively sharper resonances just as illuminating more slits produces a sharper optical diffraction pattern.

In the experiment, potassium atoms pass midway between the two plates of a parallel plate transmission line where they are excited by two dye lasers from the ground 4s state to the 21s state in a static electric field. The atoms are subsequently exposed to the rf pulse to drive the $21s \rightarrow 19,3$ transition. Finally, a field ionization pulse is applied with an amplitude sufficient to ionize the 19,3 state but not the 21s state. The ions pass through a 0.4 mm diameter hole in the upper plate of the transmission line and are detected.

To generate the short rf pulses we use a Philips PM 5785B pulse generator with clock and pulse outputs at the same frequency, typically 20 MHz. The clock output drives a step recovery diode to generate harmonics, and a Hewlett-Packard (HP) 5340B sweep oscillator is phase locked to the desired harmonic. Putting the sweep oscillator output into the local oscillator port of a mixer and the pulse generator output into the intermediate frequency port produces a train of phase-locked rf pulses at the radio frequency port. The rf pulses range from 3.5 to 100 ns long and contain integral numbers of half cycles. Using a second mixer, we select the first rf pulse after the laser pulse and amplify it. The amplified pulses are brought by 50 Ω coaxial cable to the parallel plate transmission line inside the vacuum system. To have a 50 Ω impedance in the line, the ratio of the plate width to spacing is maintained at 377/50 [10]. Where the transmission line joins the cable the plate spacing is 1 mm, and over a length 10 cm it is increased to 8.5 mm. For 22 cm this separation is maintained, and in the middle of this region the atomic beam crosses the transmission line. At the end of the parallel plate line the spacing is reduced to 1 mm over a 10 cm length and connected to a 50 Ω load.

The lower plate of the transmission line is isolated with microwave capacitors, allowing the dc voltage and ionization pulse (1 μs rise time) to be applied to it. rf pulses are attenuated by 2 dB on passing through the entire line but are not changed in shape. Using a pickup probe, we have observed small distortions in the pulse in the parallel plate section which are consistent with voltage reflection coefficients of 0.19 at the capacitors.

In Fig. 3 we show the observed and calculated 19,3 signals as functions of static field for a 454 MHz pulse of amplitude $E_{\rm rf} = 4.4$ V/cm and several pulse lengths.

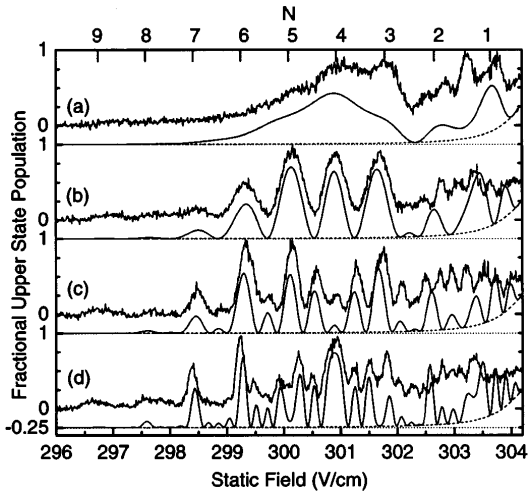

FIG. 3. Experimental and calculated signals for 454 MHz pulses of amplitude 4.4 V/cm. (a) 3/2 cycles (1 positive half cycle), (b) 5/2 cycles (2 positive half cycles), (c) 7/2 cycles (3 positive half cycles), and (d) 11/2 cycles (5 positive half cycles). The noisy curves are the experimental data. The smooth solid curves are the total calculated signals and the broken lines the calculated contribution due to excitation of the upper state at the avoided crossing. All experimental traces have been normalized to the range [0,1], and the calculations have been offset by −0.25, one scale division, for clarity.

There are two contributions to the experimental signals, the $21s \rightarrow 19,3$ transitions driven by the rf pulse and the direct laser excitation of the upper energy eigenstate as E_s approaches E_c [11]. Because of overlapping field ionization signals we cannot obtain absolute experimental transition probabilities, and the experimental traces are normalized to the calculated 19,3 signals, shown by the smooth solid curves. The portion of a calculated signal due to laser excitation of the upper energy eigenstate is shown by the broken lines [11], and the remainder is due to the rf transitions. The transition probability is calculated by computing the unitary time evolution matrix U for a single cycle and using the matrix U^M to calculate the response to M cycles. In Fig. 3(a) we show the trace obtained with a 3/2 cycle pulse, specifically a negative half cycle before and after the positive half cycle. Traces essentially identical to those shown in Fig. 3(a) are obtained with pulses containing one positive and one negative half cycle as well as only one positive half cycle. Given the energy levels shown in Fig. 1 it is not surprising that it is only the number of positive half cycles which matters. The signal monotonically increases until $E_s = 301$ V/cm, at which point the peak field $E_s + E_{\mathrm{rf}}$ slightly exceeds the avoided crossing field E_c. For larger values of E_s Stückelberg oscillations, having the origin depicted in Fig. 2(b), are clearly visible in the calculated signal. We attribute the discrepancy between the measured and calculated curves of Fig. 3(a) for $E_s = 301$ V/cm to the small reflections in the transmission line. The regime $E_{\mathrm{rf}} + E_s > E_c$, the Stückelberg oscillation regime, is particularly sensitive to the precise shape of the individual field cycle. This issue is less important in the region $E_{\mathrm{rf}} + E_s < E_c$ where the multiphoton resonances build up from many cycles.

A pulse with two positive half cycles (and three negative half cycles) produces the trace of Fig. 3(b). The most striking difference from Fig. 3(a) is that the structureless region between 297 and 301 V/cm in Fig. 3(a) now exhibits a pronounced sinusoidal modulation similar to Young's two slit interference pattern. The origin of the modulation is intercycle interference which is easily understood by referring to Fig. 2(c), which shows the time dependence of the two energy levels in a two cycle pulse for which $E_s + E_{\mathrm{rf}} = E_c$. There is a transition amplitude from the 21s to the 19,3 state on each of the field cycles resulting in the two transition pathways shown in Fig. 2(c). The amplitudes add constructively if their phase difference $\Phi = 2\pi N$ and destructively if $\Phi = 2\pi(N + \frac{1}{2})$ where N is an integer. Φ is the energy difference between the two states integrated over one cycle, i.e., the area indicated in Fig. 2(c). Since the W_{21s} and $W_{19,3}$ are constant and sinusoidally varying, respectively, $\Phi = (\overline{W}_{21s} - \overline{W}_{19,3})\tau$, where $\overline{W}_{21s}$ and $\overline{W}_{19,3}$ are the time average energies of the two states, i.e., their energies in the static field alone, and τ is the period of the rf field. Interference maxima, where $\Phi = 2\pi N$, occur for static fields at which the separation of the two levels is an integer multiple N of the rf frequency. Since the maxima occur at the fields of the N photon resonances, it is convenient to call them the resonant maxima. Note that in Fig. 3(b) the transition probability vanishes at 302.4 V/cm, as in Fig. 3(a). If the transition probability is zero after one cycle, it remains so after any number of cycles.

When there are three positive (and four negative) half cycles we obtain the trace of Fig. 3(c). Each of the resonant maxima of Fig. 3(b) becomes sharper, and an additional set of maxima appears between them. In a three slit optical experiment the new maxima would be subsidiary maxima smaller than the resonant maxima [12], and such is the case for $E_s < 300$ V/cm, where the single cycle response of Fig. 3(a) is weak. When the transition probability approaches 1 the optical analogy breaks down. For example, the $N = 4$ resonant maximum at 301 V/cm is smaller than the new maxima on either side of $E_s = 301$ V/cm. At the resonant maximum the single cycle response of Fig. 3(a) is strong enough that in only three cycles the atoms can make approximately the full Rabi oscillation from 21s to 19,3 and back to 21s again. A pulse with five positive (and six negative) half cycles leads to the trace of Fig. 3(d) in which the observed features are generally sharper than in Fig. 3(c), as might be expected. Only where the single cycle transition probability of Fig. 3(a) is small do the resonant maxima stand out clearly. The agreement in Fig. 3 between the data and the calculations, based on the method of Moloney and Meath, is evident. In addition, since the transition amplitude comes from the positive peak of the rf field, and we tune the atomic energy levels, our experiment is almost exactly analogous to ATI and may be viewed as a confirmation of Muller's model of ATI [8].

The fact that the Rabi frequency exceeds the inverse of the pulse length for much of Fig. 3 obscures an interesting point: the multiphoton transition probability in lowest order perturbation theory (LOPT) is identical to optical diffraction. If p is the $21s \rightarrow 19,3$ transition amplitude for a single cycle, the transition amplitude from the mth cycle of an M cycle pulse is $pe^{im\Phi}$ where Φ is the phase shift between cycles defined previously and shown in Fig. 2(c). In LOPT the transition probability P for the M cycle pulse is given by

$$P = \left| \sum_{m=0}^{M-1} p e^{im\Phi} \right|^2, \qquad (1)$$

precisely the same expression used to describe an optical diffraction pattern from M slits [12]. This expression is only valid for $P \ll 1$, a condition which is not well satisfied in much of Fig. 3.

The similarity to optical diffraction is more apparent in the traces shown in Fig. 4 taken with slightly higher frequency, 570 MHz, and lower amplitude, 1 V/cm. With this low field amplitude the single cycle response is weak enough that the features which develop into the two and

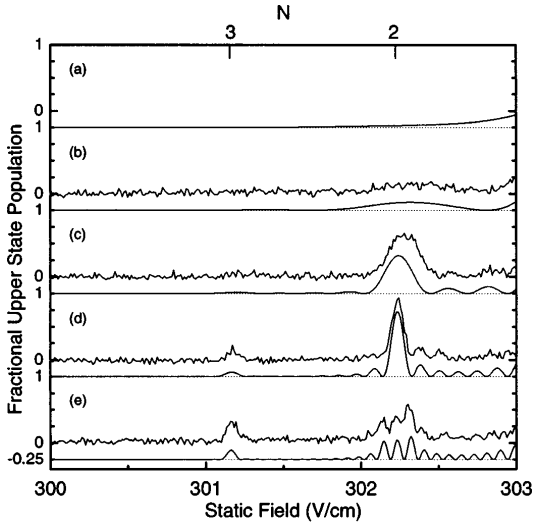

FIG. 4. Experimental and calculated transition probabilities for 570 MHz pulses of amplitude 1 V/cm. (a) 1 cycle, (b) 2 cycles, (c) 5 cycles, (d) 10 cycles, and (e) 15 cycles. As in Fig. 3 the noisy traces are the experimental data and the smooth curves the calculated transition probabilities, and the *y* axis is drawn similarly.

three photon resonances remain clearly separated. To acquire these data we excited the atoms in a static field well below the avoided crossing and brought the atoms to the static fields given in Fig. 4 with a 1 μs rise time 5 V/cm pulse, before applying the rf pulse. This procedure ensured that the observed signal was due only to the rf transition, not to laser excitation of the upper state in the anticrossing.

In Fig. 4 we show calculated curves for 1, 2, 5, 10, and 15 cycles as well as experimental curves for all but one cycle. We cannot make a single cycle pulse at 570 MHz, but as shown by Fig. 4(a), the calculated single cycle transition probability is almost structureless. As shown in Fig. 4(b), with two cycles a broad resonant maximum appears at the location of the two photon transition. With the five cycle pulse shown in Fig. 4(c) the two photon resonance is clearly visible above the adjacent subsidiary maximum on the high static field side. In addition, this subsidiary maximum is reduced in intensity from the resonant maximum by the square of the number of field cycles, as is true in an optical diffraction pattern [12]. With the ten cycle pulse of Fig. 4(d) the three photon resonance appears, and the subsidiary maxima near the two photon resonance are clearly visible but are only a factor of 10 weaker than the resonance itself, not a factor of 100 as would be the case for diffraction. LOPT and therefore the optical description are breaking down for the two photon resonance. With 15 cycles, as shown in Fig. 4(e), the three photon resonance is more visible, and the two photon resonance is broken up into a group of maxima of comparable size, indicating the complete breakdown of LOPT.

In conclusion, we have shown that as rf pulses are increased in length from one to many cycles the resulting transition probability evolves from an almost structureless function of the energy level spacing to one exhibiting the sharp features characteristic of resonance experiments. This evolution is implicit in the response to a single rf cycle and is similar to the evolution of a diffraction pattern as more slits are illuminated. The diffraction analog can direct our thinking in useful ways. For example, as pointed out by Jones [13], the analog to blazing a grating, choosing the shape of a field cycle, i.e., the phases and amplitudes of its harmonic constituents, can enhance the transition probability for specific high order transitions [14–16].

It is a pleasure to acknowledge stimulating conversation with R. R. Jones and D. W. Schumacher. This work has been supported by the Air Force Office of Scientific Research.

*Present address: Physics Division, NIST, Gaithersburg, MD 20899.

[1] G. M. Lankhuijzen and L. D. Noordam, Phys. Rev. Lett. **74**, 355 (1995).
[2] K. C. Kulander, K. J. Schafer, and J. L. Krause, in *Atoms in Intense Radiation Fields*, edited by M. Gavrila (Academic, New York, 1992).
[3] J. H. Shirley, Phys. Rev. **138**, B979 (1965).
[4] S.-I. Chu, Adv. At. Mol. Phys. **21**, 197 (1985).
[5] J. Zhou, G. Taft, C. P. Huang, M. M. Murnane, H. C. Kapteyn, and I. P. Christov, Opt. Lett. **19**, 1149 (1994).
[6] A. Stingl, M. Lenzner, Ch. Spielmann, F. Krause, and R. Szipöcs, Opt. Lett. **20**, 602 (1995).
[7] J. V. Moloney and W. J. Meath, Mol. Phys. **31**, 1537 (1976).
[8] H. G. Muller, Comments At. Mol. Phys. **24**, 355 (1990).
[9] L. A. Bloomfield, R. C. Stoneman, and T. F. Gallagher, Phys. Rev. Lett. **57**, 2512 (1986).
[10] S. Ramo, J. R. Whinnery, and T. van Duzer, *Fields and Waves in Communication Electronics* (Wiley, New York, 1984).
[11] R. C. Stoneman, G. R. Janik, and T. F. Gallagher, Phys. Rev. A **34**, 2952 (1986).
[12] M. V. Klein and T. E. Furtak, *Optics* (Wiley, New York, 1986).
[13] R. R. Jones (private communication).
[14] C. Chen and D. S. Elliot, Phys. Rev. Lett. **65**, 1737 (1990).
[15] D. W. Schumacher, F. Weihe, H. G. Muller, and P. H. Bucksbaum, Phys. Rev. Lett. **73**, 1344 (1994).
[16] V. Veniard, R. Taleb, and A. Maquet, Phys. Rev. Lett. **74**, 4161 (1995).